Evaluating the shear strength of a natural heterogeneous soil using reconstituted mixtures

- **First Online** 07 October 2016
- **DOI** https://doi.org/10.1680/jgeot.15.P.022
- **Publisher Name** ICE Publishing

Please cite this paper as:

Ruggeri P., Segato D., Fruzzetti V.M.E., Scarpelli G. (2016) Evaluating the shear strength of a natural heterogeneous soil using reconstituted mixtures. Géotechnique, 66(11), 941-946; DOI:10.1680/jgeot.15.P.022

Date: 4-2016

Title: Evaluating the shear strength of a natural heterogeneous soil using reconstituted mixtures

Authors: Paolo Ruggeri (lead author, Post-doc Researcher)

David Segato (co-author, PhD, senior engineer GES srl)

Viviene M.E. Fruzzetti (co-author, Researcher)

Giuseppe Scarpelli (co-author, Full Professor)

Affiliation: Paolo Ruggeri, Viviene M.E. Fruzzetti, Giuseppe Scarpelli

Department of Materials, Environmental Sciences and Urban Planning (SIMAU)

Università Politecnica delle Marche, Ancona, Italy

David Segato

GES srl via Brecce Bianche, 12, Ancona, Italy

Address: Paolo Ruggeri

Department of Materials, Environmental Sciences and Urban Planning (SIMAU)

Università Politecnica delle Marche

Via Brecce Bianche, Ancona, Italy

Tel. +39 071 2204231

E-mail: p.ruggeri@univpm.it

N. of words: 2216

N. of tables: 1

N. of figures: 5

Notation:

C fines content (here defined as the passing at 63 μm in % of the total weight of solids)

d_{50} mean grain size: particle size for which 50% of the particles are finer and 50% are coarser

d_{max} maximum grain size: particle size for which 95% of the particles are finer

HTP Highly Tectonized Phyllite

HTP10 Reconstituted mixtures containing grains smaller than 2 mm

HTP40 Reconstituted mixtures containing grains smaller than 0·425 mm

HTPm Matrix of HTP (grains smaller than 63 μm)

M critical state friction parameter

p' mean effective stress

p'_{cs} mean effective stress at critical state

q_{cs} deviator stress at critical state

UC uniformity coefficient, ratio of the 60% particle size to the 10% particle size

v specific volume

v_c specific volume of the fines

v_g specific volume of the granular fraction

$v_{g,max}$ maximum value of the specific volume of the granular fraction

Keywords: shear strength cohesive mixtures laboratory tests

particle packing clay

INTRODUCTION

Geotechnical characterisation of complex formations, transitional soils and heterogeneous materials requires specific care because their mechanical response is not straightforward. This is the case of a heterogeneous soil outcropping along a landslide-prone hillside where a dam shoulder had to be built. For a safe design of the dam it is necessary to pay specific attention to the slope stability, so a great effort has been devoted to the soil characterisation. The soil originated from a large tectonic strain deformation of the weak rock which produced a mélange of grain particles enclosed in fine grey matrix, geologically identified as Highly Tectonized Phyllite (henceforth denoted as HTP). The tectonic origin of the soil indicates that the variability in gradation of grains and fines content have to be taken into account. Moreover, the presence of a significant coarse fraction makes it difficult to core undisturbed samples.

Considering these issues, an unconventional approach, based on an extensive series of drained triaxial compression tests on reconstituted samples was attempted (Ruggeri, 2008). Three mixture suites were reconstituted and tested by varying particle grading and maximum grain size. Then, leading from the framework outlined in literature for studies on binary mixtures (Fragatzy *et al,* 1992; Irfan e Tang, 1992; Wood and Kumar, 2000; Jafari and Shafiee, 2004; Monkul and Ozden, 2007), the results were elaborated and interpreted to identify and quantify the key parameters which govern the mechanical response of analysed mixtures. These outcomes allow us to estimate the shear strength of natural HTP by knowing its grading curve and to consider the effect of grading variation.

According to several authors (Picarelli and Olivares, 1998; Cotecchia *et al.*, 2015), the behaviour of structurally complex formation at the scale of landslide is governed by a strength varying between residual and constant volume friction angle. These observations support the relevance of strength evaluated on reconstituted samples for the investigated HTP.

MATERIALS, METHODOLOGY AND APPROACH

Visual inspection of HTP core samples shows heterogeneity of the granular composition, even if the matrix appeared enough to enclose every coarse grain. The representative HTP grading curve (Fig. 1), evaluated on a large amount of soil, exhibits the presence of 8% clay, 27% silt, 37% sand and 28% gravel, and its shape indicates a poorly graded soil, lacking in fine sand fraction. The fine particle distribution is very close to a fractal limiting grading well represented by the Fuller curve with d_{max} = 0·3 mm. Such outcomes are consistent with the origin of the soil. Soils subjected to high tectonic stresses are typically poorly graded, deficient in specific ranges of the particle sizes and with a finer grain distribution matching the Fuller curve as demonstrated by applying fractal analysis to a different geological process (Sammis *et al.*, 1986; Sornette *et al.*, 1990; Prosperini and Perugini, 2008).

Lack of fine sand and the self-similar distribution attained for the finer grains prompted us to assimilate the investigated soil to a binary mixture assuming the grain matrix to be smaller than 63μm. On the basis of this assumption, natural HTP was composed of 35% of matrix and 65% of granular fraction. The pure matrix, named HTPm, was composed of 78% silt and 22% clay.

Atterberg limits were determined on the pure matrix by obtaining a liquid limit of 30 and a plastic limit of 18.

Experimental programme

Three differently graded mixtures were tested, namely HTP, HTP10 and HTP40. The HTP series contained grains smaller than 16 mm which well represents the particle distribution of natural soil. The HTP10 series only contained the grains passing the ASTM10 sieve (average diameter 2 mm), and the HTP40 series only contained the grains passing the ASTM40 sieve (average diameter 0·425 mm). In this way, with HTP10, the behaviour of mixtures containing sand-silt-clay fractions (without gravel fraction) is studied while, with the HTP40, the soil fraction conventionally used for fine soil classification (i.e., Atterberg limits) is considered.

For each of the above mixtures, a set of ten samples were reconstituted with different matrix contents quantified by the digits at the end of the test identification code (HTP/0-90, HTP10/0-90 and HTP40/0-90). Moreover, additional tests were carried out on the reconstituted samples of pure matrix. In Figures 2a, b and c, the grading curves for the considered mixtures are shown.

Due to the dimension of the grains, the HTP series was tested on large size samples (170 mm height, 84 mm diameter) so that the ratio between the sample diameter and max grain size turns out to be larger than 5 (Head, 1992); on the contrary, standard size samples (76 mm height, 38 mm diameter) were considered for HTP10 and HTP40 series.

Sample preparation

The natural soil was wet sieved and oven dried. The granular fraction was divided into three parts which were graded differently: part A retained all the fractions, part B and part C only the grains passing the ASTM10 and ASTM40 sieves, respectively.

The different mixtures were then prepared by adding granular parts A, B or C with the matrix in the desired proportions. Two different procedures were used to set up the reconstituted samples. For mixtures containing a low proportion of matrix, the samples were set up directly on the pedestal of the triaxial cell following the wet pluviation method for sand specimens (Head, 1992, granular sample preparation). On the contrary, when the matrix was sufficient to enclose grains, each mixture was mixed thoroughly with a quantity of distilled water equal to approximately 100% of the dry weight of the matrix. The obtained slurry was poured in a consolidation cylinder of diameter equal to the required triaxial sample, consolidated at 200 kPa of vertical stress, extruded and trimmed to the exact height and set up on the triaxial cell (cohesive sample preparation).

Testing equipment

Triaxial testing was carried out by using two different apparatuses. The first apparatus, used for standard size samples, was a Bishop & Wesley-type stress path triaxial cell, supplied with three pressure/volume controllers, fully computerised. The second apparatus, for larger samples, was a standard triaxial testing equipment with cell and back pressures supplied by pressure/volume actuators. Every sensor has an appropriate Full Output Scale (FSO) and accuracy which is generally better than 0·1% of FSO.

Test scheme

The samples were tested with porous stones at both ends, and no measure was taken in order to reduce end friction. All samples were saturated, consolidated to an isotropic effective stress of 400 kPa (selected considering the effective stress acting on the sliding plane of the landslides identified in the valley) and then axially compressed at a constant axial strain rate of 0·47%/h. The axial compression was typically stopped at an axial strain of 20 percent, after which the sample was unloaded and dismantled.

Strains were estimated with the assumption that the samples maintain their shape during axial compression. Evidently, this hypothesis becomes less accurate for large strains, when samples tend to barrel.

In order to evaluate the specific volume at critical state, accurate measurements of initial water content and water content after dismantling were carried out. The normally consolidated condition of the samples guarantees the meaningfulness of the global void ratio at failure evaluated by water content measurement of the entire sample (Desrues, 1996).

Definition of key parameters

Assuming an ideal saturated mixture comprised of water, fines (matrix) and granular skeleton, the fines content (C) is defined as:

$$C = \frac{m_{\mathrm{c}}}{m_{\mathrm{c}} + m_{\mathrm{g}}} \tag{1}$$

(where m_{c} is the mass of fine fraction and m_{g} is the mass of granular fraction).

If the specific gravities of matrix and granular fraction are similar, as is acceptable in this case, the value of the previous parameter does not change if expressed in terms of volumes. Thus, according to Wood and Kumar (2000), in addition to the specific volume (v), it is possible to define the granular specific volume (v_{g}) and the fines specific volume (v_{c}) as:

$$v_{\mathrm{g}} = \frac{V_{\mathrm{w}} + V_{\mathrm{c}} + V_{\mathrm{g}}}{V_{\mathrm{g}}} = \frac{v}{1 - C} \tag{2}$$

$$v_{\mathrm{c}} = \frac{V_{\mathrm{w}} + V_{\mathrm{c}}}{V_{\mathrm{c}}} = \frac{v + C - 1}{C} \tag{3}$$

where V_{w}, V_{c} and V_{g} are the volumes of water, fine and coarse grains, respectively.

An exhaustive description of the physical meaning of these variables can be found in Thevanayagam and Mohan (2000) where an intuitive framework to describe the behaviour of silty sands is presented. Note that in a grain-sustained condition, v_{c} has no physical meaning because the fines are not necessarily uniformly distributed in the sample, and large voids could be present. Vice versa, in a matrix-sustained condition, v_{c} is representative of the mean density of fines.

RESULTS AND DISCUSSION

Table 1 summarizes the data of the triaxial tests carried out for the present study. Plots of the stress ratio and volumetric strain against axial strain are presented in Figure 3. None of the stress-strain plots present a significant peak, and a critical state failure condition is always achieved. From the final values of the stress invariants, the critical state parameter $M = (q/p')_{cs}$ was evaluated.

These values of M are plotted in Figure 4 with the corresponding fines content C for the three tested series, HTP, HTP10 and HTP40. Generally, as expected, it is observed that friction decreases as the fines content increases for all the test series. The HTP series at a fines content of 35%, representative of the average condition of the natural soil, shows an M value of 1·26 (31°); at the same fines content, the HTP10 and HTP40 indicate an M value of 1·30 (32°) and 1·33 (33°), respectively. Note that the variation in shear strength is small and that, unexpectedly, the HTP series (containing the entire granular fraction of natural soil) exhibits the minimum value of friction, while the HTP40 series (containing only grains passing 425 μm sieve) shows the maximum friction. Moreover, the friction of the HTP series decreases more rapidly than that of the HTP10 and HTP40 ones as fines content increases.

In order to investigate such behaviour, the trends of global specific volume of the different mixtures, together with the corresponding trends of grain packing in terms of granular specific volume (v_g) and fines specific volume (v_c) at critical state, have been plotted in Figure 5. The three plots of the specific volume (v) match the expected pattern with an initial decrease followed by its increase with the increase in the fines content.

Granular specific volume (v_g) coincides with v for purely granular samples, then v_g rises rapidly with the increase in the fines. On the three plots of granular specific volume, with a star symbol, the maximum values of the specific volume for the granular fraction alone ($v_{g,max}$) of the three tested series are also indicated, evaluated according to ASTM D4253 and ASTM D4254; it can be observed how these values are close to the minimum of the respective curve of the global specific volume. When the granular specific volume of a mixture exceeds the maximum granular specific volume of its granular fraction, intergranular contacts cease to be effective, and the grains start to separate, marking the transition from a grain-sustained to a matrix-sustained behaviour.

Fines specific volume curves decrease when C increases, asymptotically reaching the value of the global specific volume of the pure matrix samples (C = 100%). For C values beyond approximately

50-70% (earlier for graded mixtures, i.e., HTP, later for uniform mixtures, i.e., HTP40), v_c at failure becomes constant for all the tested series.

These findings put the trends of M-plots in Figure 4 in a different light: well graded mixtures (i.e., HTP) have little maximum specific volume, so they can accommodate less fines in the voids and a modest amount of fines allows them to reach a matrix-sustained condition and a low friction angle; on the contrary, uniform mixtures (i.e., HTP40) have a large maximum specific volume, so they can accommodate much fines in the voids and an important amount of fines is required to separate the grains allowing them to obtain a decrease in friction.

CONCLUSIONS

The influence of the grading and coarse grain dimensions on the strength characteristics of the Highly Tectonized Phyllite (HTP) was analysed by drained triaxial compression tests on reconstituted samples and interpreted using the framework established in the literature for binary mixtures. Based on the work presented in this paper, the following conclusions are drawn:

a) Soils subjected to high tectonic stresses typically show a gap in the grading curve and develop a distribution of fine particles coinciding with the self-similar distribution; this gives a practical criterion to rationally identify the matrix of natural heterogeneous soils.

b) The critical state friction of the reconstituted HTP mixture, having the same composition of natural soil, can be estimated as $M = 1{\cdot}26$ (31°). Taking in mind that natural HTP appears generally matrix sustained, it can be concluded that its M value is slightly influenced by limited variation of fines content and grading of the granular fraction.

c) In a matrix sustained field, a gradual decrease in friction was observed with an increase in the fines content.

d) Grading of the granular part governs the amount of fines needed to determine a transition from a grain-sustained to a matrix-sustained behaviour.

e) Maximum granular specific volume and fines content (C) associated with maximum density are the key parameters to identify the transition threshold of mixtures.

In light of these findings, the procedure outlined in this paper can represent a way to estimate the critical state friction of heterogeneous, matrix-sustained soils in order to overcome the difficulties of undisturbed sampling and to obtain a conscious estimate of geotechnical parameters.

Figure 1. Particle size distribution of natural HTP soil compared with fractal distribution traced with $d_{max} = 0{\cdot}3$ mm

Figure 2. Particle size distributions of tested samples: a) HTP, b) HTP10, c) HTP40 series

Figure 3. Stress ratio and volumetric strain against axial strain response for tested mixtures at different fines content: a) HTP, b) HTP10, c) HTP40 series

Figure 4. Critical state parameter M against fines content C for the tested series

Figure 5. Plots of specific volumes v, v_g and v_c for the tested series

Table 1. Summary of laboratory tests on HTP mixtures, including: the preparation technique adopted; the fines content C; the initial water content w_0; the global void ratio $v^{(1)}$ and mean effective stress p' at the end of the isotropic compression stage; the values of global specific volume at failure, $v^{(2\text{-}i)}$ and $v^{(2\text{-}f)}$, related to initial and final water content; the granular $v_g^{(2\text{-}f)}$ and matrix specific volume $v_c^{(2\text{-}f)}$ at failure evaluated from the final water content w_f; stress invariants and their ratio at critical state (M).

REFERENCES

Cotecchia, F., Vitone, C., Santaloia, F., Pedone, G., Bottiglieri, O. (2015) Slope instability processes in intensely fissured clays: case histories in the Southern Apennines. *Landslides* **12**: 877-893

Desrues, J., Chambon, R., Mokni, M. & Mazerolle, F. (1996). Void ratio evolution inside shear bands in triaxial sand specimens studied by computed tomography. *Géotechnique* **46**(3):529-546.

Fragaszy, R. J., Su, J., Siddiqi, F. H., Ho, C. L. (1992). Modeling strength of sandy gravel. *Journal of Geotechnical Engineering, ASCE* **118**(6): 920-935.

Fuller, W. B. and Thompson, S. E. (1907). The laws of proportioning concrete, *Transactions of ASCE*, ASCE, **59**, 67-143.

Georgiannou, V. N., Hight, D. W. & Burland, J. B. (1990). The undrained behaviour of clayey sands in triaxial compression and extension. *Géotechnique* **40**(3): 431-449.

Head , K. H. (1992). *Manual of soil laboratory testing*. 2nd edn. Wiley, London, 1998.

Irfan, T. Y. & Tang, K. Y. (1993). *Effect of the coarse fraction on the shear strength of colluviums*. Geot. Eng. Office, Civil Eng. Dept., Hong Kong Government, Hong Kong, Report No.23.

Jafari, M. K. & Shafiee, A. (2004). Mechanical behaviour of compacted composite clays. *Canadian Geotechnical Journal* **41**(6): 1152-1167.

Lade, P. V., Liggio, C. D., Jr. & Yamamuro, J. A. (1998). Effect of Non-Plastic Fines on Minimum and Maximum Void Ratios of Sand. *Geotechnical Testing Journal* **21** (4): 336-347.

McDowell, G. R., Bolton, M. D. & Robertson, D. (1996). The fractal crushing of granular materials. *J. Mech. Phys. Solids* **44**, No.12, 2079-2102.

Monkul, M. M., Ozden, G. (2007). Compressional behavior of clayey sand and transition fines content. *Engineering Geology* **89**, 195-205.

Newman, K. (1959). The effect of water absorption by aggregates on the water/cement ratio of concrete. *Magazine of Concrete Research* **11**, No.33, 135-142.

Ni, Q., Tan, T. S., Dasari G. R., Hight, D. W. (2004). Contribution of fines to the compressive strength of mixed soils. *Géotechnique* **54**(9): 561-569.

Picarelli L. & Olivares L. (1998) Ingredients for modelling the mechanical behaviour of intensely fissured clay shales. In: The geotechnics of hard soils - soft rocks. Proceedings of the second international symposium on hard soils-soft rocks, Naples, October 1998. (Two volumes), pp. 771-780. ISBN: 9058090183

Prosperini, N. and Perugini, D. (2008). Particle size distributions of some soils from the Umbria Region (Italy): fractal analysis and numerical modelling. *Geoderma* **145**(3-4): 185-195. doi:10.106/j.geoderma.2008.03.004.

Ruggeri, P. (2008). Comportamento meccanico di un terreno complesso a granulometria eterogenea. *Ph.D. Thesis*, Università Politecnica delle Marche, Ancona, Italy (in Italian).

Sammis, C., Osborne, R., Anderson, J., Banerdt, M., White, P. (1986). Self-similar cataclasis in the formation of fault gouge. *Pure and Applied Geophysics* **125**, 777-812

Sornette, A., Davy, P., Sornette, D. (1990). Growth of fractal fault patterns. *Physical Review Letters* **65**, 2266-2269

Thevanayagam, S. & Mohan, S. (2000). Intergranular state variables and stress-strain behaviour of silty sands. *Géotechnique* **50**(1), 1-23.

Thevanayagam, S. (1998). Effect of fines and confining stress on undrained shear strength of silty sands. *J. Geotech. Geoenviron. Engng Div., ASCE* **124**(6), 479-491.

Vallejo, L. E. (2001). Interpretation of the limits in shear strength in binary granular mixtures. *Canadian Geotechnical Journal* **38**(5), 1097-1104.

Wood, D. M. & Kumar, G. V. (2000). Experimental observations of behaviour of heterogeneous soils. *Mech. Cohes.-Frict. Mater.* **5**, 373-398.

Figure 1

Click here to download Figure ruggeri_fig1.xlsx

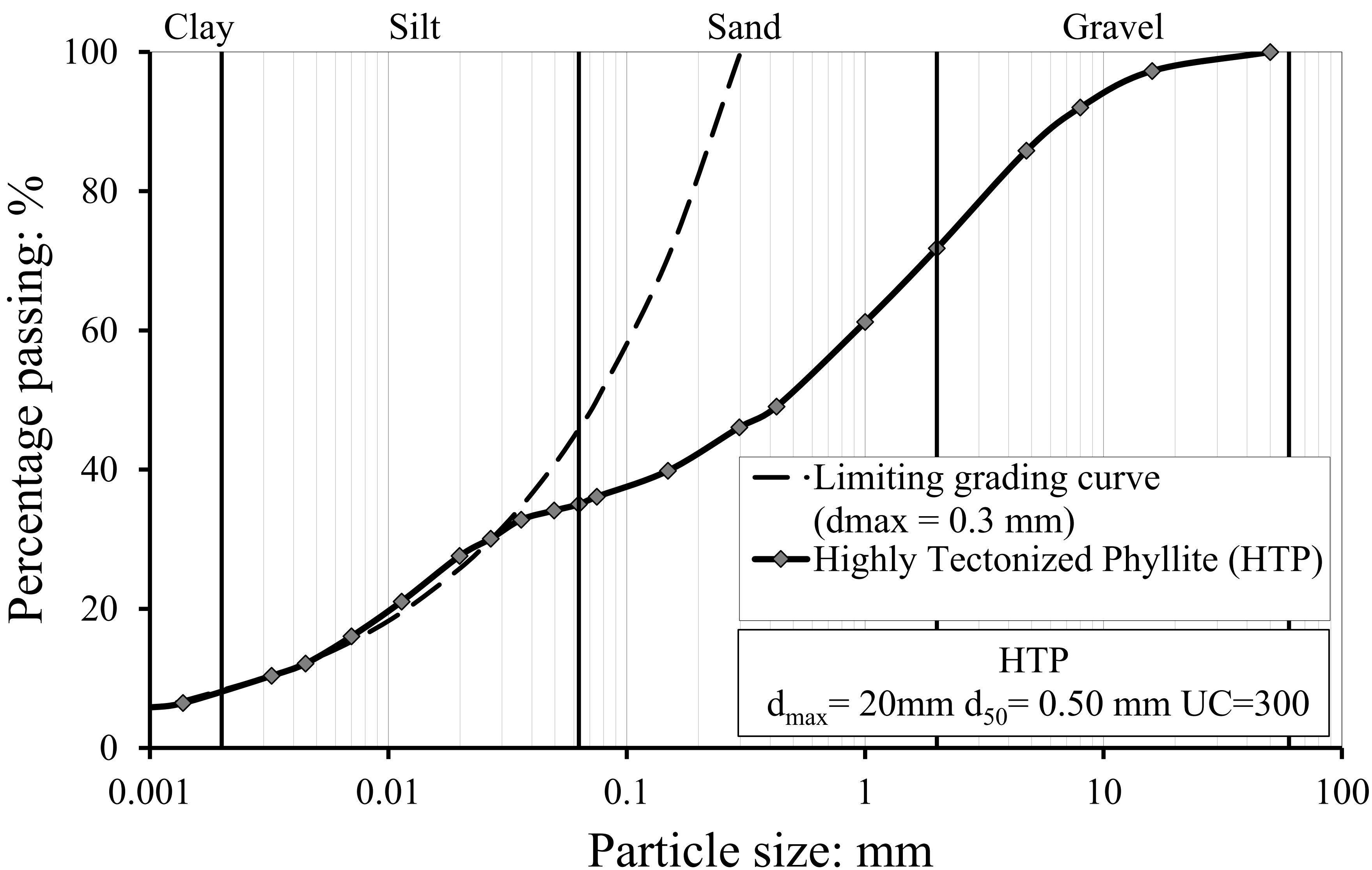

Figure 2a

Click here to download Figure ruggeri_fig2a_rev.xlsx

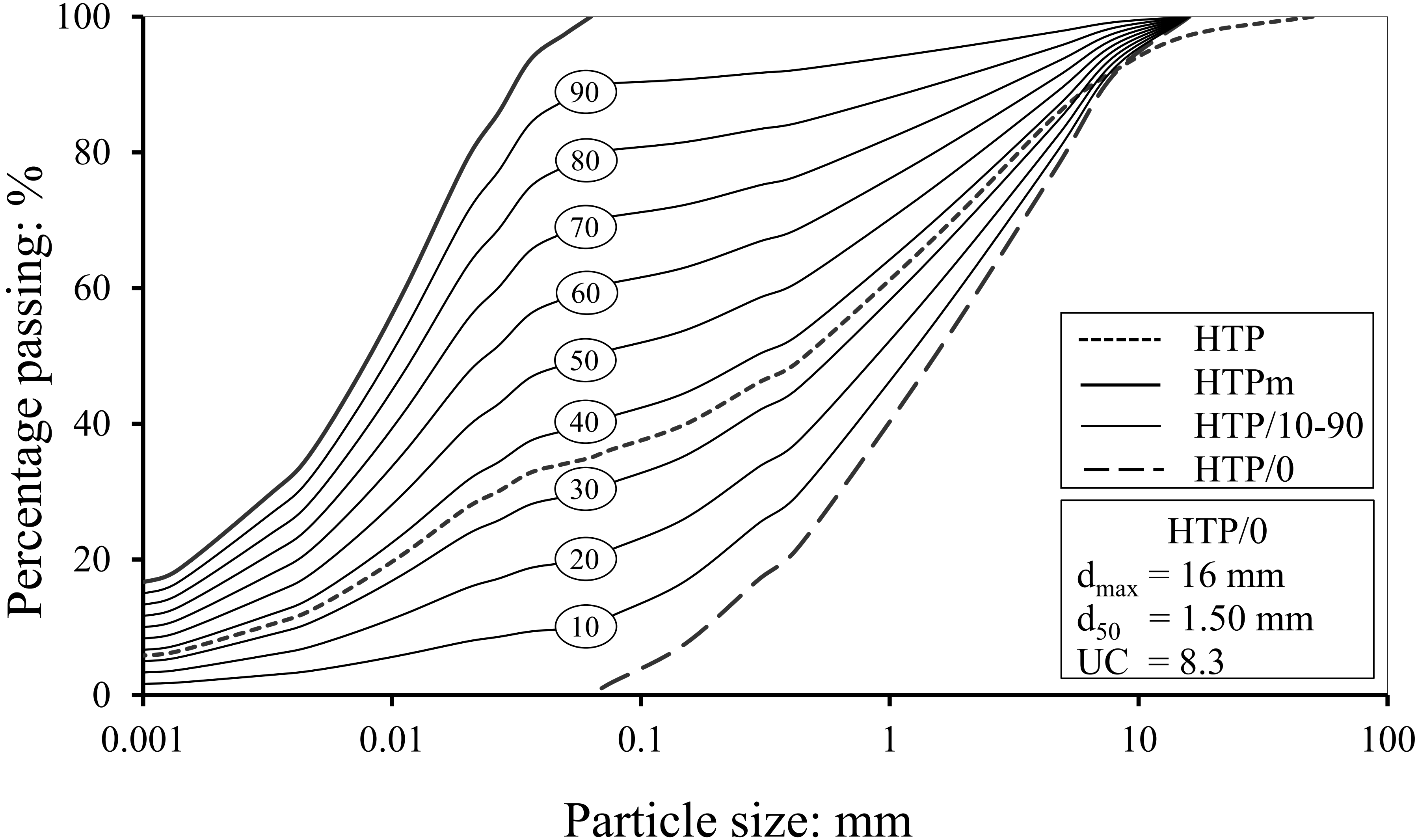

Figure 2b

Click here to download Figure ruggeri_fig2b_rev.xlsx

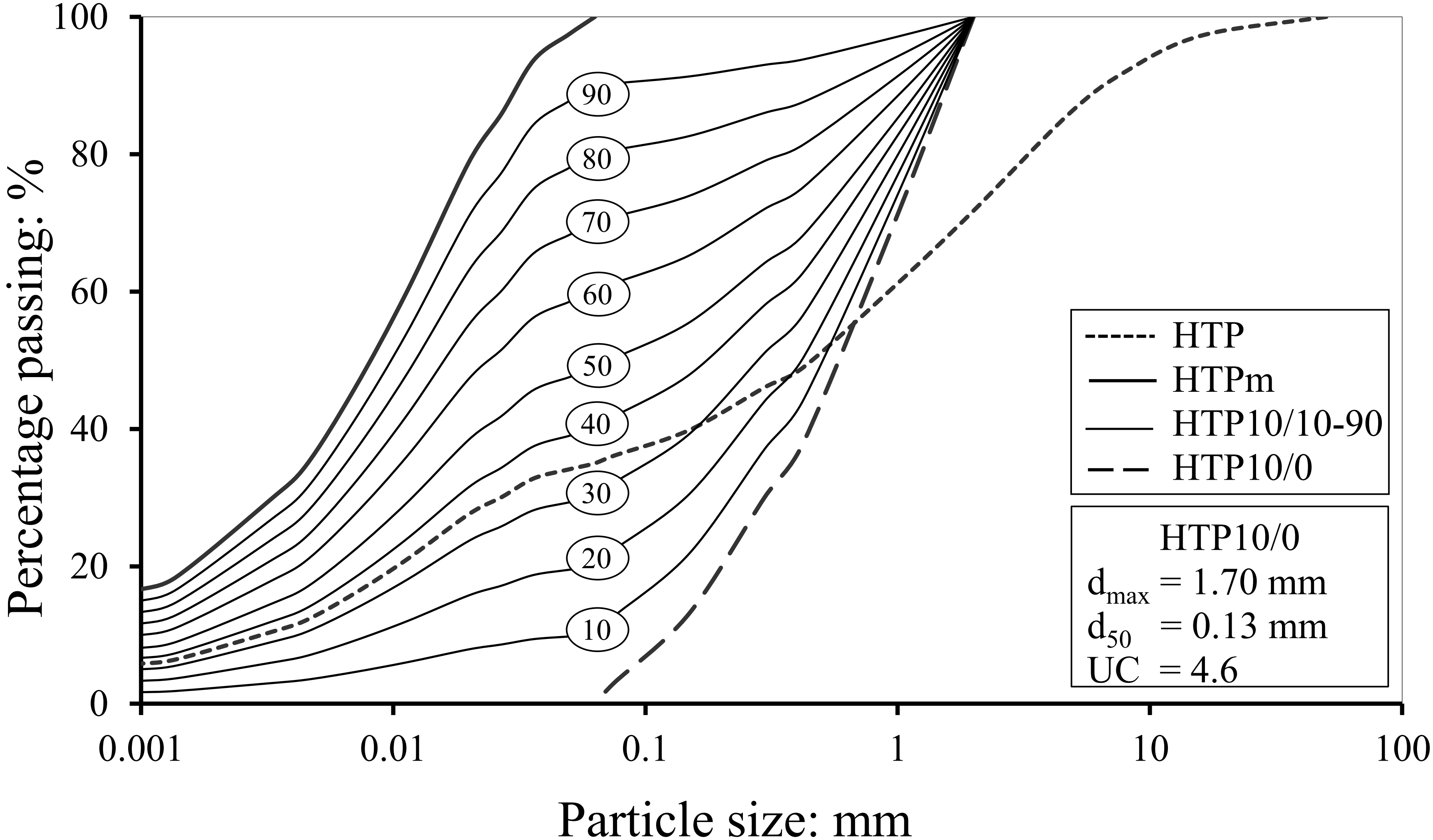

Figure 2c

Click here to download Figure ruggeri_fig2c_rev.xlsx

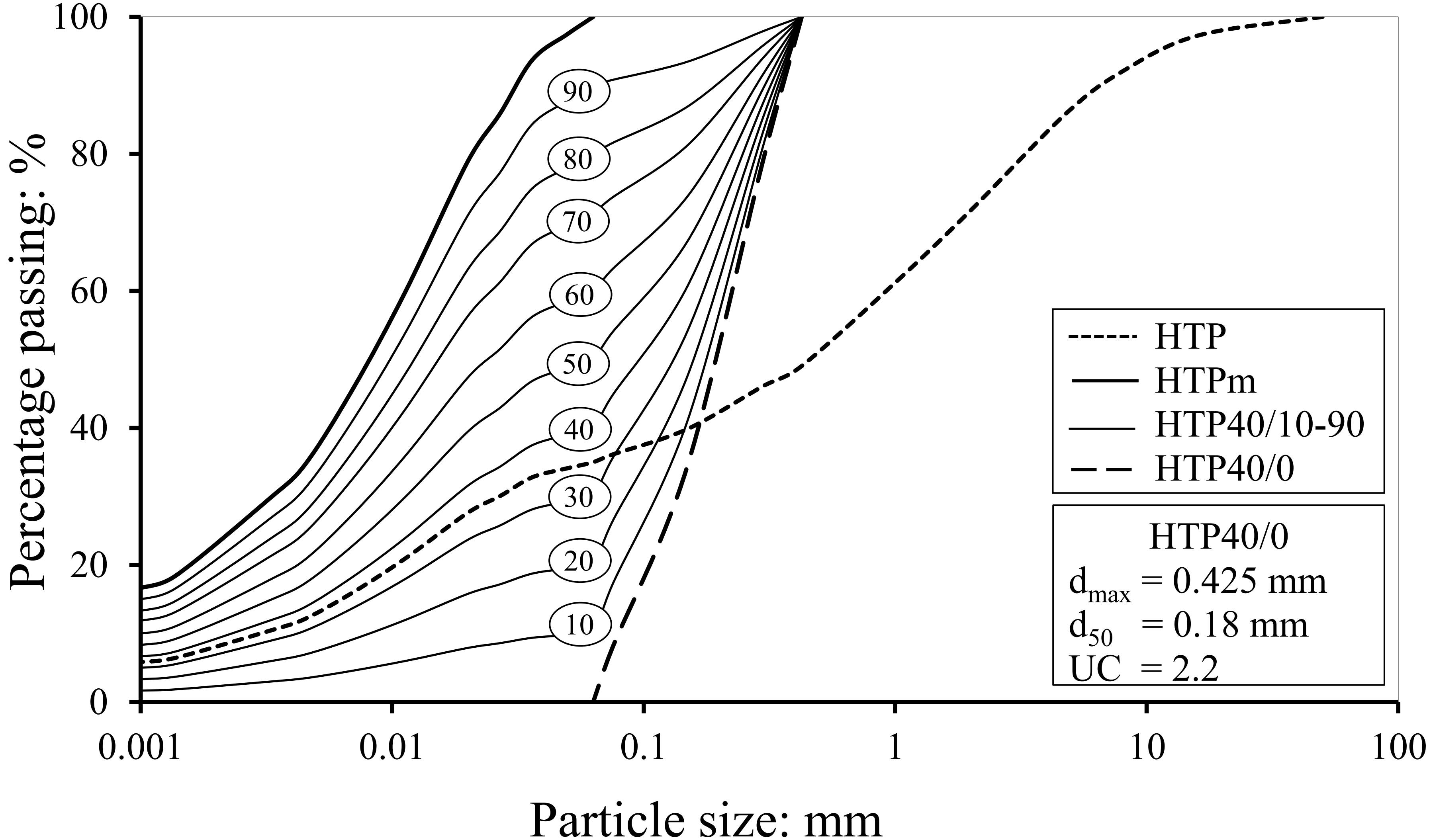

Figure 3a

Click here to download Figure ruggeri_fig3aN.xlsx

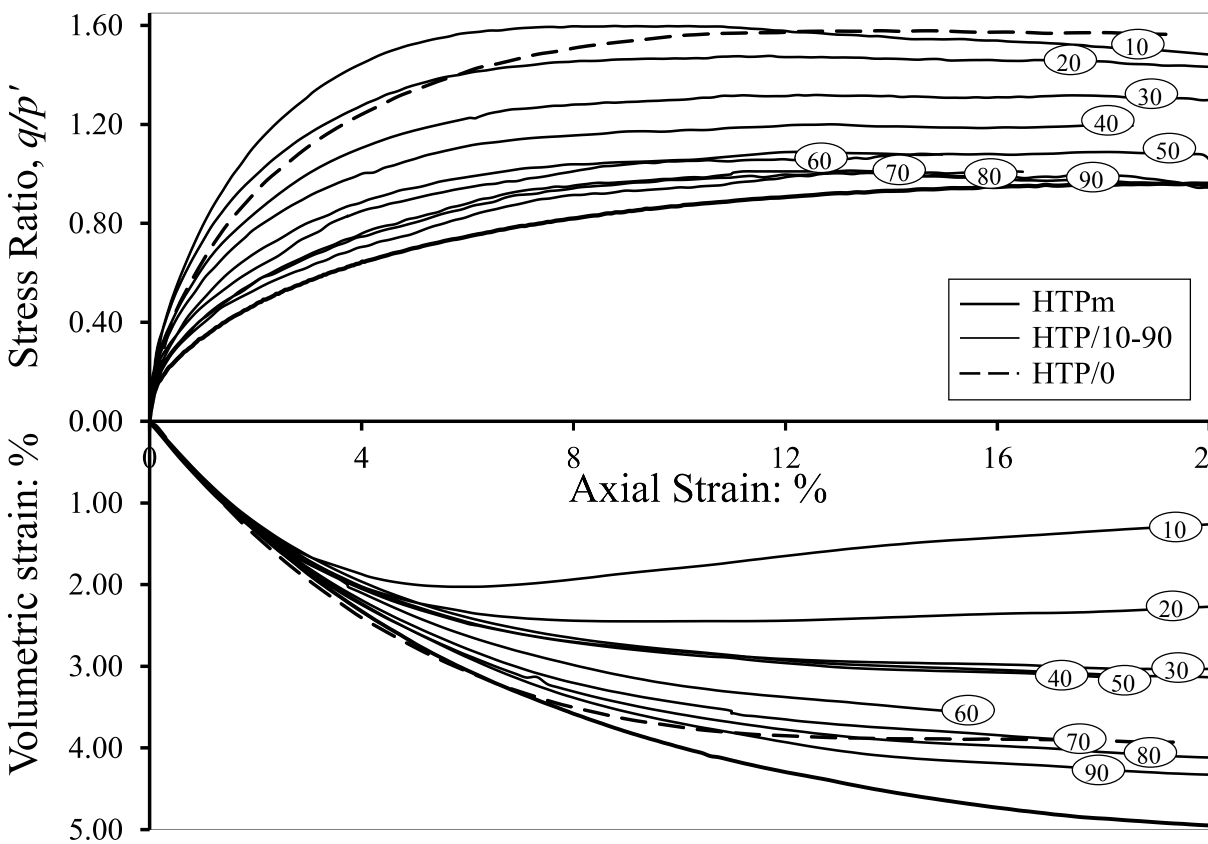

Figure 3b

Click here to download Figure ruggeri_fig3bN.xlsx

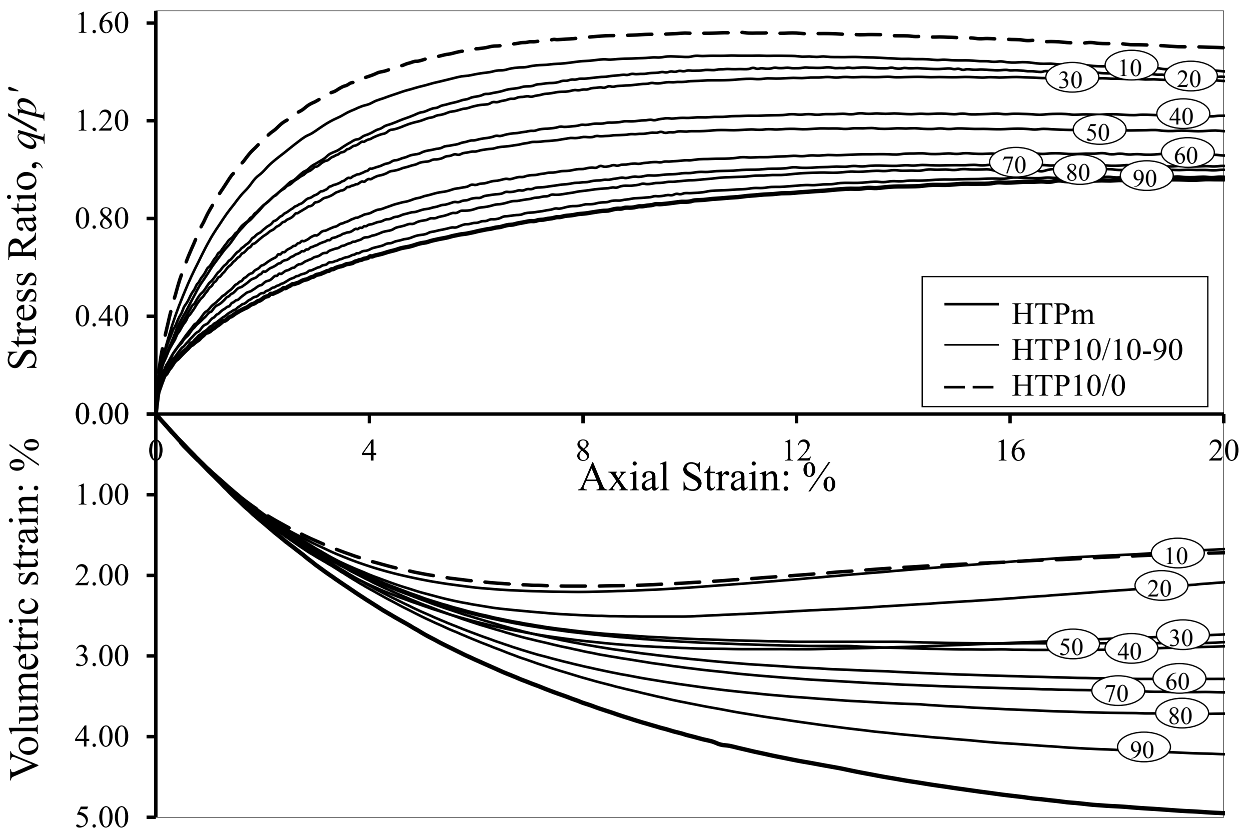

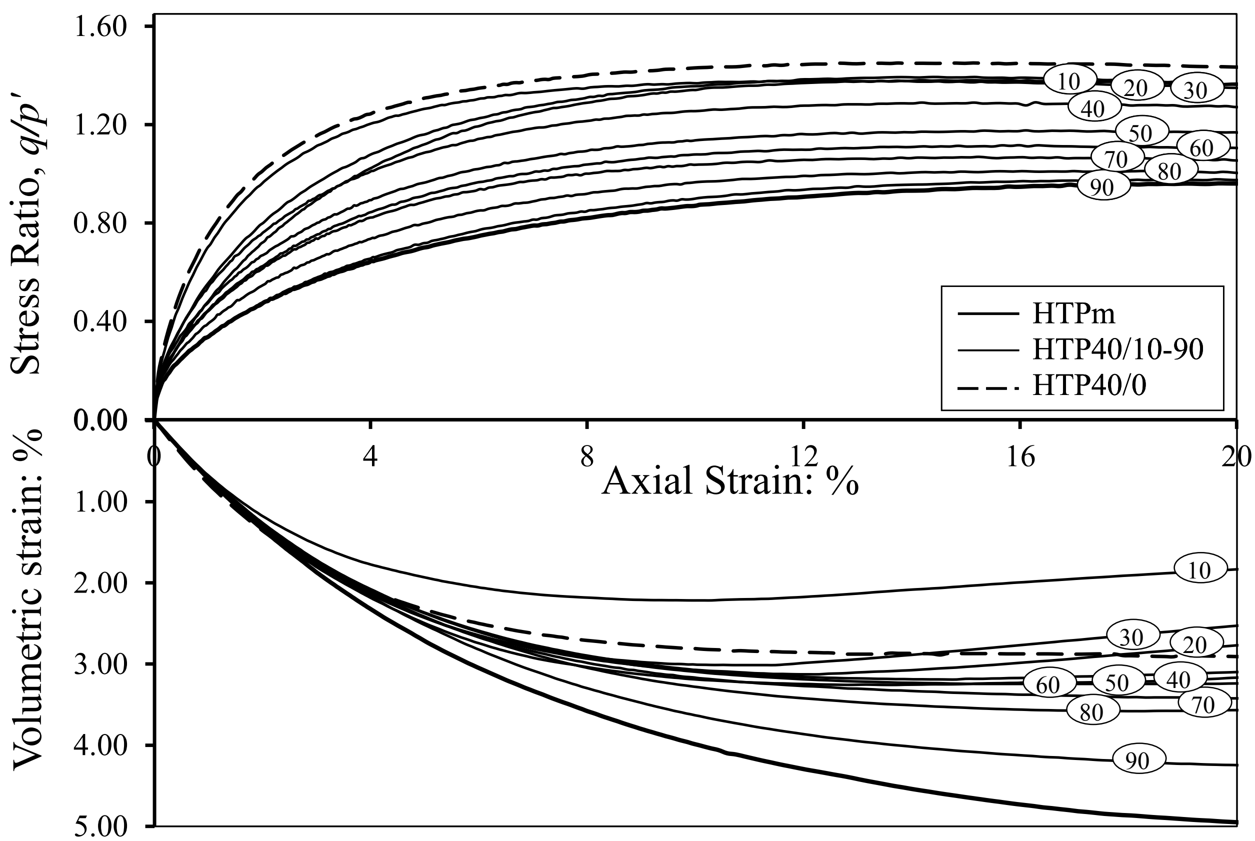
Stress Ratio, q/p'
1.60
1.20
0.80
0.40
0.00
10
20
30
40
50
60
70
80
90
HTPm
HTP40/10-90
HTP40/0
0
4
8
12
16
20
Axial Strain: %
Volumetric strain: %
1.00
2.00
3.00
4.00
5.00

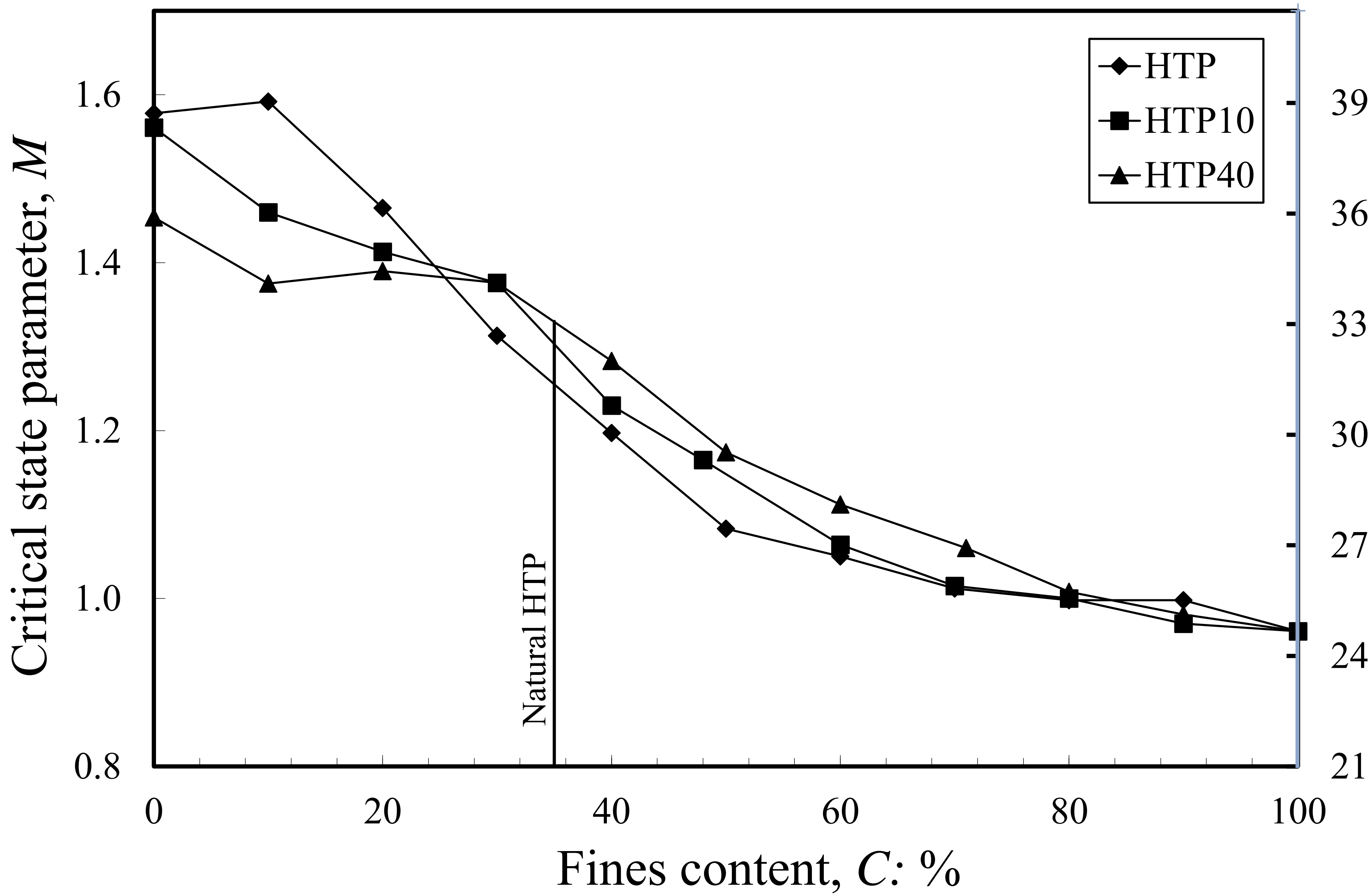

HTP
HTP10
HTP40
Natural HTP
Critical state parameter, M
Fines content, C: %
1.6
1.4
1.2
1.0
0.8
0
20
40
60
80
100
39
36
33
30
27
24
21

Figure 5

Click here to download Figure ruggeri_fig5N.xlsx

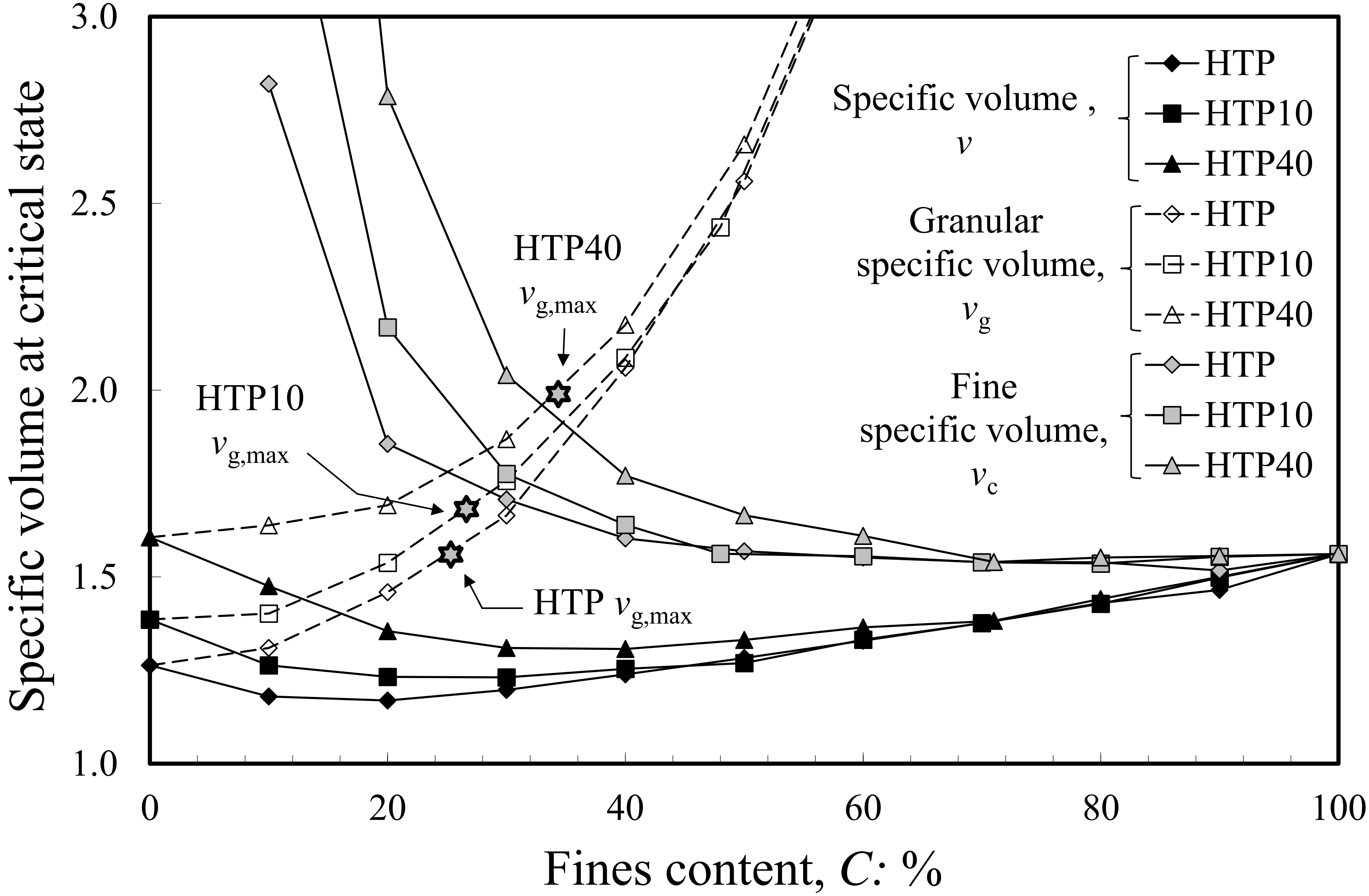

Test code	Sample preparation	C: %	w_0: %	End of consolidation		At critical state								
				$v^{(1)}$	p': kPa	$v^{(2\text{-}i)}$	w_f: %	$v^{(2\text{-}f)}$	$v_g^{(2\text{-}f)}$	$v_c^{(2\text{-}f)}$	p'_{cs}: kPa	q_{cs}: kPa	M	φ_{cs}'
HTP/0	Granular	0	-	-	400	-	10·5	1·263	1·263	-	834	1316	1·578	38·7
HTP/10	Granular	10	-	-	400	-	7·4	1·180	1·310	>10	849	1352	1·592	39·0
HTP/20	Cohesive	20	9·8	1·193	400	1·165	6·9	1·169	1·459	1·856	778	1140	1·465	36·1
HTP/30	Cohesive	30	11·8	1·224	400	1·186	7·8	1·197	1·664	1·707	706	927	1·313	32·6
HTP/40	Cohesive	40	13·0	1·285	400	1·243	9·2	1·239	2·060	1·603	660	790	1·197	29·9
HTP/50	Cohesive	50	14·6	1·333	400	1·291	10·7	1·283	2·559	1·569	624	676	1·083	27·3
HTP/60	Cohesive	60	17·1	1·385	400	1·335	12·2	1·329	3·315	1·552	616	663	1·050	26·5
HTP/70	Cohesive	70	19·2	1·430	400	1·373	13·8	1·376	4·578	1·540	596	603	1·012	25·7
HTP/80	Cohesive	80	21·8	1·475	400	1·413	15·6	1·430	7·139	1·539	592	591	0·998	25·3
HTP/90	Cohesive	90	23·2	1·508	400	1·440	16·7	1·465	>10	1·517	585	584	0·998	25·3
HTP10/0	Granular	0	-	-	400	-	14·6	1·386	1·386	-	836	1305	1·561	38·3
HTP10/10	Granular	10	-	-	400	-	10·1	1·263	1·402	3·645	780	1139	1·460	36·0
HTP10/20	Granular	20	-	-	400	-	8·9	1·232	1·538	2·168	757	1070	1·413	34·9
HTP10/30	Cohesive	30	12·1	1·250	400	1·221	8·8	1·231	1·757	1·776	740	1018	1·376	34·0
HTP10/40	Cohesive	40	13·1	1·288	400	1·253	9·6	1·254	2·087	1·639	678	834	1·230	30·7
HTP10/50	Cohesive	48	13·9	1·296	400	1·261	10·0	1·269	2·436	1·562	655	763	1·165	29·2
HTP10/60	Cohesive	60	16·3	1·365	400	1·319	12·2	1·332	3·325	1·555	621	661	1·064	26·9
HTP10/70	Cohesive	70	18·3	1·420	400	1·370	13·7	1·376	4·581	1·539	606	615	1·015	25·7
HTP10/80	Cohesive	80	21·2	1·463	400	1·407	15·5	1·428	7·135	1·536	600	600	1·000	25·4
HTP10/90	Cohesive	90	24·9	1·574	400	1·505	17·9	1·498	>10	1·554	592	574	0·970	24·7
HTP40/0	Granular	0	-	-	400	-	22·6	1·606	1·606	-	776	1128	1·454	35·8
HTP40/10	Granular	10	-	-	400	-	17·8	1·475	1·638	5·782	739	1016	1·375	34·0
HTP40/20	Granular	20	-	-	400	-	13·4	1·355	1·692	2·787	747	1038	1·390	34·4
HTP40/30	Cohesive	30	15·1	1·321	400	1·310	11·7	1·310	1·869	2·040	740	1018	1·376	34·0
HTP40/40	Cohesive	40	15·5	1·343	400	1·303	11·5	1·307	2·175	1·771	700	898	1·283	31·9
HTP40/50	Cohesive	50	15·6	1·350	400	1·310	12·2	1·331	2·658	1·665	657	771	1·174	29·4
HTP40/60	Cohesive	60	17·9	1·402	400	1·358	13·4	1·365	3·407	1·610	636	707	1·112	28·0
HTP40/70	Cohesive	71	19·1	1·419	400	1·371	13·9	1·382	4·761	1·540	621	658	1·060	26·8
HTP40/80	Cohesive	80	21·0	1·475	400	1·422	15·9	1·441	7·198	1·552	604	609	1·008	25·6
HTP40/90	Cohesive	90	24·5	1·560	400	1·491	18·0	1·500	>10	1·556	594	583	0·981	24·9
HTPm	Cohesive	100	26·9	1·618	400	1·537	20·0	1·561	-	1·561	590	567	0·961	24·5